Published in final edited form as:
Mol Imaging Biol. 2012 December ; 14(6): 735–742. doi:10.1007/s11307-012-0552-4.

Tumor dosimetry using [^{124}I]m-iodobenzylguanidine microPET/CT for [^{131}I]m- iodobenzylguanidine treatment of neuroblastoma in a murine xenograft model

Youngho Seo[1,2,3], **W. Clay Gustafson**[4], **Shorouk F. Dannoon**[1], **Erin A. Nekritz**[4], **Chang-Lae Lee**[5], **Stephanie T. Murphy**[1], **Henry F. VanBrocklin**[1], **Miguel Hernandez-Pampaloni**[1], **Daphne A. Haas-Kogan**[2,6], **William A. Weiss**[4,6,7], and **Katherine K. Matthay**[4]

[1]Department of Radiology and Biomedical Imaging, University of California, San Francisco, CA 94143, USA

[2]Department of Radiation Oncology, University of California, San Francisco, CA 94143, USA

[3]UC Berkeley – UCSF Graduate Program in Bioengineering, University of California, Berkeley and San Francisco, CA 94143, USA

[4]Department of Pediatrics, University of California, San Francisco, CA 94143, USA

[5]Department of Radiological Science and Research Institute of Health Science, Yonsei University, Wonju, Korea

[6]Department of Neurological Surgery, University of California, San Francisco, CA 94143, USA

[7]Department of Neurology, University of California, San Francisco, CA 94143, USA

Abstract

Purpose—[^{124}I]m-iodobenzylguanidine (^{124}I-mIBG) provides a quantitative tool for pretherapy tumor imaging and dosimetry when performed before [^{131}I]m-iodobenzylguanidine (^{131}I-mIBG) targeted radionuclide therapy of neuroblastoma. ^{124}I ($T_{1/2}$=4.2d) has a comparable half-life to that of ^{131}I ($T_{1/2}$=8.02d), and can be imaged by PET for accurate quantification of the radiotracer distribution. We estimated expected radiation dose in tumors from ^{131}I-mIBG therapy using ^{124}I-mIBG microPET/CT imaging data in a murine xenograft model of neuroblastoma transduced to express high levels of the human norepinephrine transporter (hNET).

Procedures—In order to enhance mIBG uptake for in vivo imaging and therapy, NB 1691-luciferase (NB1691) human neuroblastoma cells were engineered to express high levels of hNET protein by lentiviral transduction (NB1691-hNET). Both NB1691 and NB1691-hNET cells were implanted subcutaneously and into renal capsules in athymic mice. ^{124}I-mIBG (4.2–6.5 MBq) was administered intravenously for microPET/CT imaging at 5 time points over 95 hours (0.5, 3–5, 24, 48, and 93–95 h median time points). In vivo biodistribution data in normal organs, tumors, and whole-body were collected from reconstructed PET images corrected for photon attenuation using the CT-based attenuation map. Organ and tumor dosimetry were determined for ^{124}I-mIBG. Dose estimates for ^{131}I-mIBG were made, assuming the same in vivo biodistribution as ^{124}I-mIBG.

Results—All NB1691-hNET tumors had significant uptake and retention of ^{124}I-mIBG, whereas unmodified NB1691 tumors did not demonstrate quantifiable mIBG uptake *in vivo*, despite *in vitro* uptake. ^{124}I-mIBG with microPET/CT provided an accurate 3-dimensional tool for estimating the radiation dose that would be delivered with ^{131}I-mIBG therapy. For example, in our

Correspondence to: Youngho Seo, Ph.D.; telephone: 1-415-353-9464; fax: 1-415-353-9421; youngho.seo@ucsf.edu.

Conflict of interest disclosure. The authors declare no conflict of interests.

model system, we estimated that the administration of ^{131}I-mIBG in the range of 52.8 – 206 MBq would deliver 20 Gy to tumors.

Conclusion—The overexpression of hNET was found to be critical for ^{124}I-mIBG uptake and retention in vivo. The quantitative ^{124}I-mIBG PET/CT is a promising new tool to predict tumor radiation doses with ^{131}I-mIBG therapy of neuroblastoma. This methodology may be applied to tumor dosimetry of ^{131}I-mIBG therapy in human subjects using ^{124}I-mIBG pretherapy PET/CT data.

Keywords

neuroblastoma; m-iodobenzylguanidine; iodine-124; iodine-131; PET/CT; animal model; radiation dosimetry

Introduction

Neuroblastoma is derived from embryonic sympathetic nervous tissue and is the most common extracranial pediatric solid cancer [1, 2]. Patients with advanced neuroblastoma have a very poor prognosis, particularly for those who become resistant to conventional treatment [3].

M-iodobenzylguanidine (mIBG) is an aralkylguanidine norepinephrine analogue, and has been labeled with radioiodines [4, 5] for imaging and therapy. [^{123}I]m-iodobenzylguanidine (^{123}I-mIBG) has been used for planar and single photon emission computed tomography (SPECT) imaging to detect tumors of the sympathetic nervous system such as neuroblastoma and pheochromocytoma [6]. 2-deoxy-2-[^{18}F]fluoro-D-glucose (^{18}F-FDG) positron emission tomography (PET), which provides better three dimensional localization but is less tumor specific, has recently been reported to be a sensitive imaging agent for neuroblastoma and other pediatric solid tumors [7, 8]. Approximately 90% of neuroblastomas are mIBG-avid, so that labeled mIBG is now recommended as the most specific indicator for staging and response evaluation in neuroblastoma [6, 9, 10]. [^{131}I]m-iodobenzylguanidine (^{131}I-mIBG) emits beta particles locally, and has also become part of standard retrieval therapy of neuroblastoma, with 30–40% response rate in relapsed disease [1, 11].

In order to improve the efficacy of this targeted radionuclide therapy, investigators have tested increasing the dose with rapid sequence double infusion, and combining the radiotherapy with chemotherapy or radiosensitizers [12–14]. We recently showed that vorinostat, a histone deacetylase inhibitor with preclinical efficacy in neuroblastoma, may be synergistic with radiotherapy in a murine xenograft model, and also increases expression of the human norepinephrine transporter, thereby increasing mIBG uptake [15, 16]

The lack of neuroblastoma xenograft models with *in vivo* uptake of mIBG has hindered further exploration of combination therapies, and also made correlation with tumor dosimetry in these models difficult. Most previously published studies using mIBG in murine models have utilized nonneuroblastoma tumor cell lines transduced with the hNET, in order to facilitate uptake. In the past, murine models of neuroblastoma or human xenograft models have rarely been used to test ^{131}I-mIBG therapy due to poor mIBG uptake *in vivo* by many of the neuroblastoma cell lines despite human norepinephrine transporter (hNET) expression and good *in vitro* uptake. For this reason, other tumor types transduced with hNET have been used to examine mIBG uptake and therapy [17, 18].

Although I-131 itself can be imaged with SPECT, I-131 imaging using conventional SPECT cameras has significant technical limitations [19] and is time-consuming at the multiple time

points required to estimate radiation dose. For targeted radionuclide therapy using I-131, accurate pretherapy dosimetry would allow tailoring of the tumor dose and minimizing normal organ toxicity. Previous studies in patients with tumor dosimetry of ^{131}I-mIBG have shown wide variability using the conjugate planar method [20]. Other newer variations using SPECT have been proposed but not yet validated [21]. We showed previously that preclinical [^{124}I]m-iodobenzylguanidine (^{124}I-mIBG) PET/CT (PET combined with computed tomography) in mice could produce organ radiation dose estimates of clinical ^{131}I-mIBG therapy, and ^{124}I-mIBG PET imaging could be administered without significant internal radiation dose burden in pediatric patients with neuroblastoma [22]. However, in our previous work, we only showed how the ^{124}I-mIBG distributes to organs in animal models that did not have any tumor uptake. It is necessary now to estimate the radiation dose for normal organs when there is significant tumor uptake of mIBG, and also estimate the radiation dose to the neuroblastoma tumors. We used I-124, a positron-emitting radionuclide for mIBG imaging studies because ^{124}I-PET provides more accurate radionuclide quantification capabilities than ^{131}I-SPECT when an optimized energy window setting to capture 511 keV annihilation photons is applied so that the contamination of high energy gammas from I-124 decays is minimized [23]. In addition, I-124 has a comparable half-life (4.2 days) to that of I-131 (8.02 days) so that the pharmacokinetics of mIBG uptake and retention in living animals may be measured, permitting more accurate radiation dose estimation in tumors.

In this report, we use a murine xenograft model with a human neuroblastoma cell line that has been transduced with the hNET for better mIBG uptake, and show the utility of *in vivo* imaging validation of ^{124}I-mIBG tumor uptake and dosimetry in a preclinical model of neuroblastoma using PET-CT scans.

Materials and Methods

^{124}I-mIBG

All imaging experiments in this paper were performed using iodine-124 (purchased from IBA Molecular, Sterling, VA) labeled mIBG (precursors provided by Molecular Insight Pharmaceuticals, Cambridge, MA). The I-124 labeling was performed as previously published with some modifications [24] The polymer precursor (~0.5 mg) was swelled in 300 μL of ethanol for at least 15 min. To the reaction vial containing the swelled polymer was added sequentially 100 μL of 0.1 M $KHPO_4$, 35–50 μL of (37–74) MBq of I-124 in 0.002 M NaOH, 450–465 μL of distilled water (the final volume of I-124 and water should add up to 500 μL), and 100 μL of the oxidation solution (1.68:1 30% H_2O_2:acetic acid). The reaction took place at room temperature and was vortexed occasionally. After 2 hours the reaction was quenched with 200 μL of 0.1 M $NaHSO_3$. The reaction mixture was passed through a syringe filter, and loaded on to a preconditioned C18 light SepPak. The SepPak was washed with water then eluted with ethanol fractions. The fractions with the highest amount of activity were combined and placed under N_2 flow to evaporate. Saline was added to give the final working solution. The final product was analyzed by RP-HPLC (Waters 600 Controller connected with NaI radiation detector and UV lab alliance model 525 detector) under the following conditions: 20/80 acetonitrile/0.01 M KH_2PO_4 isocratic solvent at a flow of 1 mL/min on Phenomenex Luna 5 μ C18 column. The radiochemical purity was over 99% prior to administration of the labeled ^{124}I-mIBG into animals.

^{124}I-mIBG in vitro studies

The labeled ^{124}I-mIBG was evaluated *in vitro* using NB1691 neuroblastoma cells which had been previously modified to express the firefly luciferase protein (NB1691) [25, 26]. The complementary deoxyribonucleic acid (cDNA) for hNET was cloned by polymerase chain

reaction (PCR) into the pLenti6.3-V5 expression plasmid (Invitrogen, Carlsbad, CA). Virus was generated per manufacturers protocol, NB1691 cells were transduced and stable selectants were obtained by blasticidin selection (NB1691-hNET). The hNET in these cells is not regulated transcriptionally to avoid downregulation in tumor growth. The tumors overexpressing hNET also had a c-terminal epitope tag that was used to verify the hNET overexpression with a commonly available V5 antibody by western blotting (Invitrogen, Carlsbad, CA). In addition to NB1691, and NB1691 cells, nonneuronal NIH 3T3 and human embryonic kidney (HEK) 293T cells that do not express hNET were used as control for *in vitro* evaluation of ^{124}I-mIBG. Approximately 0.7 MBq of ^{124}I-mIBG in 30 L of phosphate buffer saline (PBS) was added to 5×10^5 cells in triplicates for each cell line. After incubating for 2 hours at 37 °C with 5% CO_2, the cells were centrifuged and the media were removed and washed three times with a cold PBS. The cell-associated activity was measured by a gamma counter (1480 WIZARD 3", Perkin Elmer, Waltham, MA). ^{124}I-mIBG uptake was evaluated both before and after blocking with added imipramine (20 μg), a known NET blocking agent [27].

Animal models of neuroblastoma

A total of six athymic mice (weighing approximately 25 g each) were implanted subcutaneously with 1×10^6 NB1691 cells on both shoulders. In each animal, the left shoulder was injected with unmodified NB1691 cells, while the right shoulder was injected with NB1691-hNET cells. In addition, four of these six mice were injected in the left renal capsules with 1×10^6 NB1691 cells that were unmodified (n=2) or were transduced to overexpress hNET (n=2). The growth of renal capsule implants were substantially slower than that of subcutaneous implants, so three additional athymic mice were implanted with 1×10^6 NB1691 cells overexpressing hNET in the renal capsule in the left kidney to better visualize uptake in an abdominal tumor.

Animal imaging protocol

Preclinical PET/CT imaging utilized standard operating procedures approved by the University of California, San Francisco Institutional Animal Care and Use Committee (IACUC) and Laboratory Animal Resource Center (LARC). The thyroid was blocked with 0.250 mg/100 μL of an aqueous solution of sodium iodide, to prevent excessive iodine-124 uptake, administered intravenously via tail vein 1 hour prior to ^{124}I-mIBG injections.

The nine mice received 4.2–6.5 MBq of ^{124}I-mIBG solution in 100 μL volume intravenously using a custom mouse tail vein catheter with a 28-gauge needle and a 100–150 mm long polyethylene microtubing (0.28 mm I.D. × 0.64 mm O.D., Scientific Commodities, Inc., Lake Havasu City, AZ). The mice were imaged on a dedicated small animal PET/CT scanner (Inveon, Siemens Healthcare, Malvern, PA). The energy window for iodine-124 PET was set at 250–650 keV for the optimal noise equivalent count rate (NECR) performance at the given administered dose levels and the scanner characteristics [28]. All nine animals were imaged at five time points after the radiotracer administration (0.5, 3–5, 24, 48, and 93–95 h) for 60 minutes at each time point except at the 93–95 h time point. The PET data were acquired for 90 minutes at the last time point. The CT data were acquired for all five time points without removing the animals from the scanner after the PET data acquisition. The coregistration between PET and CT images was obtained using the rigid transformation matrix from the manufacturer-provided scanner calibration procedure since the geometry between PET and CT remained constant for each of PET/CT scans using the combined PET/CT scanner. Animals were anesthetized with gas isoflurane at 2% concentration mixed with medical grade oxygen. PET data were framed dynamically for the first two time points. The durations of the 0.5-h PET data were: 10×10s, 5×40s, 1×300s, and 5×600s. The 3–5 h PET data were also divided to two 1800s frames. The in vivo CT

parameters were 120 projections of continuous rotations to cover 220° with an x-ray tube operated at 80 kVp, 0.5 mA, and 175 ms exposure time.

Manufacturer-provided ordered subsets expectation maximization (OS-EM) algorithm was used for PET reconstruction that resulted in 128×128×159 matrices with a voxel size of 0.776×0.776×0.796 mm^3. The CT image was created using a conebeam Feldkamp reconstruction algorithm (COBRA) provided by Exxim Computing Corporation (Pleasanton, CA). The matrix size of the reconstructed CT images was 512×512×662 with an isotropic voxel size of 0.191×0.191×0.191 mm^3. The photon attenuation correction was performed for PET reconstruction using the coregistered CT-based attenuation map to ensure the quantitative accuracy of the reconstructed PET data.

Tumor uptake and dosimetry

Tumor and normal organ *in vivo* biodistribution studies were performed using the reconstructed PET/CT image data. The normal organ and tumor radiation dosimetry was performed for all nine animals as follows.

First, the AMIDE software package [29] was used to draw volumes of interest (VOIs) on the coregistered CT images for each tumor and organs, and VOIs were transferred to PET images. For all five time points, the same manual VOI drawing procedure was repeated using the CT images that were coregistered by applying the precalibrated rigid transformation matrix between the fixed positions of PET and CT. Once transferred apparent partial volume spill-outs were adjusted manually. For the tumors subcutaneously implanted on the shoulders of mice, the partial volume errors were minimal because there is no neighboring organ having any significant mIBG uptake.

Second, the radiation dose estimates in organs and tumors were performed using OLINDA|EXM 1.1 (Vanderbilt University, Nashville, TN) [30]. As input data required for the OLINDA|EXM software, the residence times were derived from the PET/CT images, and extrapolated to the residence times in organs of a 73.7 kg human adult subject following the method shown in Waxler SH and Enger M [31]. For the renal capsule tumor-bearing mice, doubles of the values in the nontumor-bearing kidney were used to account for both kidneys. The tumor radiation dose estimates were performed using a sphere tumor model. The excised tumors from all nine animals were round and mostly elliptical, and the assumption of the spherical volume for tumor dosimetry was not far from the actual geometrical shape. The radiation dose was first calculated for ^{124}I-mIBG, and the radiation dose expected from ^{131}I-mIBG was calculated assuming the same biodistribution between the two chemically identical radiotracers. Since the OLINDA|EXM 1.1 software only provides the dose estimates (mGy/MBq) discretely for the representative sphere mass in the linear range from 0.01 to 6000 g, for the specific weight of each tumor, the interpolated value for the dose estimate was obtained using the linear squares fit to logarithmic values of the sphere mass and the radiation dose estimate.

In addition, for visual representation of the tumor uptake of ^{124}I-mIBG, we took the 93–95 h time point PET/CT images for all nine animals we studied. At this time point, most of mIBG uptake in other organs and tissues were cleared from the animals, and the mIBG bound to hNET-overexpressing tumors was most visible. Instead of a 2-dimensional representation of mIBG uptake such as cross-sectional views, a full 3-dimensional volume rendering of both PET and CT overlaid was created using Amira (Visage Imaging, San Diego, CA).

Results

^{124}I-mIBG in vitro evaluation

The uptake of ^{124}I-mIBG in control and neuroblastoma cell lines was measured *in vitro* (Fig. 1a). Non-neural NIH 3T3 and HEK 293T cells, which do not express NET, were used as negative controls. In NB1691 cells, uptake correlated with exogenous expression of hNET as measured by western blot (Fig. 1b). We have shown previously that unmodified NB1691 cells express basal levels of hNET and take up mIBG *in vitro* [16]. The endogenous hNET is not evident in the western blot, which is only showing exogenously expressed, V5 tagged hNET. Overexpression of hNET clearly shows significant increase in mIBG uptake over unmodified NB1691 cells (Fig. 1a). Uptake was blocked by pre-treatment with imipramine, which specifically blocks norepinephrine transporters, further indicating specificity. Collectively, these data show that hNET overexpression significantly and specifically increases the *in vitro* uptake of ^{124}I-mIBG.

^{124}I-mIBG uptake in NB1691 tumors in animal models

In order to establish an *in vivo* model for mIBG dosimetry and therapy, we established xenograft tumors with both NB1691 and NB1691-hNET. Figs. 2 and 3 illustrate three-dimensional volumetric renderings of PET overlaid onto CT images with the whole mouse view, showing significant ^{124}I-mIBG uptake in the hNET-transduced cells implanted in both subcutaneous xenografts and renal capsule implants. There was no detectable mIBG uptake in subcutaneous xenografts of unmodified NB1691 tumors (Fig. 2, left shoulder) and minimal or no uptake in renal capsule implants with unmodified cells (Fig. 2, animals #3 and #4). Tumor growth in renal capsule xenografts was significantly slower than with subcutaneous tumors (Fig. 2), making simultaneous visualization of both large subcutaneous and large renal capsule tumors difficult. However, when large NB1691-hNET renal capsule tumors were established alone, clear abdominal tumor uptake of mIBG was visualized (Fig. 3). At the 93–95 h time point, most of ^{124}I-mIBG uptake in other organs and tissues was cleared from animals. The lack of *in vivo* uptake in the unmodified NB1691 is in contrast to the *in vitro* cell studies which exhibit some uptake in unmodified NB1691 cells (Fig. 1); however, it is clear in these studies that overexpression of hNET is a requirement for the enhanced uptake of mIBG in our murine xenograft model.

Radiation dose estimates in tumors

Radiation dose to organs and tumors was estimated by importing the temporal distribution data (Fig. 4) into OLINDA|EXM 1.1. The temporal change of ^{124}I-mIBG whole-body distribution is also illustrated in Fig. 5 using representative PET/CT three-dimensional volume renderings over 95 hours obtained from one animal that has a NB1691-hNET tumor. Since the OLINDA|EXM only utilizes the human models for radiation dose estimation, the results of normal organ dosimetry extrapolated to those in adult human subjects using the residence times derived from the PET/CT images in these tumor-bearing mice were shown in Table 1. Whole-body effective doses using the International Commission on Radiological Protection (ICRP) 60 tissue weighting factors are relatively smaller for the renal capsule tumor-bearing mice (0.238±0.061 mSv/MBq) than those for subcutaneous tumor-bearing mice (0.351±0.027 mSv/MBq). In order to calculate the necessary activity to administer for the therapeutic amount of ^{131}I-mIBG, we used the results from OLINDA|EXM 1.1 calculated for ^{124}I-mIBG to estimate the radiation dose estimates for ^{131}I-mIBG. The masses of excised tumors were measured after the last time point. Tumors with hNET overexpression weighed in the range of 0.08–1.84 g. For example, the calculated results from OLINDA|EXM 1.1 combined with the measured masses of the excised tumors indicated that the administration of ^{131}I-mIBG in the range of 52.8 – 206 MBq (1.43 – 5.57 mCi) would deliver 20 Gy of radiation dose to these tumors.

Hence, using this animal model that was implanted with NB1691-hNET tumors in either shoulders or renal capsules, it will be also feasible to perform ^{131}I-mIBG therapy studies given the range of ^{131}I-mIBG administration. Table 2 lists the details of the tumor dosimetry results including the tumor mass measurements from the nine animals studied.

Discussion

We have shown in this study that a human neuroblastoma cell line transduced with hNET to overexpress the norepinephrine transporter provides a reliable *in vivo* model for mIBG imaging and therapy. This cell line may be used as an intravenous metastatic model [16], subcutaneous or renal capsule model. We have shown the feasibility of organ and tumor dosimetry using the novel ^{124}I-mIBG microPET/CT imaging for both subcutaneous and renal capsule locations. These two different anatomic xenograft models confirm the importance of hNET overexpression for strong *in vivo* mIBG uptake and, more importantly, allow the establishment of an *in vivo* model system with strong mIBG uptake necessary for radiation dosimetry and therapeutic preclinical trials.

Two major questions must be answered to prove that our experimental approach using ^{124}I-mIBG in animal models of neuroblastoma will be useful in the clinical translation to improve the ^{131}I-mIBG therapy regimen. The first is whether the animal data will be faithfully reproduced in the human body. We have recently submitted an Investigational New Drug (IND) application to the US Food and Drug Administration (FDA) to initiate a clinical trial of ^{124}I-mIBG pretherapy imaging for the patients who will undergo ^{131}I-mIBG therapy. Hence, our method will be tested in the situation where the human data will be available for dosimetry and response. In comparison to ^{131}I-mIBG SPECT-based organ, whole-body, and tumor dosimetry as reported previously by Buckley et al. [21], ^{124}I-mIBG PET-based pretherapy dosimetry as we are proposing can be done with much lower radiation dose that that of the ^{131}I-mIBG therapy dose. And, ^{124}I-mIBG PET-based dosimetry will likely provide more quantitatively accurate results because of the inherent statistical improvement of photon statistics from PET over that from SPECT.

The second question is whether there is the equivalence of biodistributions between ^{124}I-mIBG and ^{131}I-mIBG uptakes *in vivo*. How accurately do the biodistribution data of ^{124}I-mIBG tumor uptake reflect the uptake of ^{131}I-mIBG within tumors? We have indirect evidence that these two chemically identical radiotracers do correspond to each other as published in our previous work [22]. The direct evidence could be obtained using both ^{131}I-mIBG and ^{124}I-mIBG in the same animal models so that the one-to-one correlation can be verified. However, ^{131}I imaging, the accuracy of in vivo biodistribution data over time might not be as good as that of ^{124}I because the quantitative accuracy of ^{131}I-mIBG imaging using SPECT is generally poorer than that of ^{124}I-mIBG imaging using PET. In addition, ^{131}I-mIBG therapy will utilize a relatively low specific activity of radioactive mIBG with presence of the cold carrier molecule, iobenguane, a biogenic amine. The selective active uptake of iobenguane by the NET expressed on the neuroendocrine cell surfaces is a competitive process. Hence, the presence of “cold” carrier iobenguane molecules could diminish the uptake in the target organs including tumors. To address this issue, it is necessary to study two cohorts of subjects, using either the carrier-added or the no-carrier-added ^{124}I-mIBG, and compare the *in vivo* biodistribution from the two datasets to evaluate the effect on normal organ and tumor dosimetry [32]. Moreover, the ultimate evaluation will require careful response assessment of measurable soft tissue lesions in patients who receive pretherapy ^{124}I-mIBG dosimetry and ^{131}I-mIBG therapy so that we can obtain the information on how tumors respond to the therapy predicted by the pretherapy dosimetry. However, the tumor response will also depend on factors not related to the radiation dose, such as variations in radiation sensitivity and heterogeneity of the tumor and stromal tissue.

Conclusion

The hNET expression correlated with ^{124}I-mIBG uptake in animal xenograft subcutaneous and orthotopic models of neuroblastoma. The tumor dosimetry for ^{131}I-mIBG was possible when the ^{124}I-mIBG uptake was followed in tumors for over 95 hours. The same method is directly translatable to neuroblastoma patients who receive pretherapy ^{124}I-mIBG PET/CT prior to the ^{131}I-mIBG treatment. In addition, the quantitative tool of ^{124}I-mIBG PET/CT and the animal model system are promising approaches to improving preclinical evaluations of ^{131}I-mIBG therapy of neuroblastoma in combination with new drug candidates.

Acknowledgments

This work was supported in part by the V Foundation (K.K.M.), National Cancer Institute under grant K25 CA114254 (Y.S.) and R01 CA154561 (Y.S.), BAERI of KRF funded by MEST grant 2011-0006368 (C.L.L.), National Cancer Institute grant R01 CA102321 (W.A.W.), P01 CA081403 (W.A.W. and K.K.M.), Dougherty Foundation (K.K.M.), and Alex Lemonade Foundation (K.K.M. and W.A.W.).

References

1. DuBois SG, Matthay KK. Radiolabeled metaiodobenzylguanidine for the treatment of neuroblastoma. Nucl Med Biol. 2008; 35(Suppl 1):S35–S48. [PubMed: 18707633]
2. Mueller S, Matthay KK. Neuroblastoma: biology and staging. Curr Oncol Rep. 2009; 11:431–438. [PubMed: 19840520]
3. Matthay KK, Villablanca JG, Seeger RC, et al. Treatment of high-risk neuroblastoma with intensive chemotherapy, radiotherapy, autologous bone marrow transplantation, and 13-cis-retinoic acid Children's Cancer Group. N Engl J Med. 1999; 341:1165–1173. [PubMed: 10519894]
4. Short JH, Darby TD. Sympathetic nervous system blocking agents. 3. Derivatives of benzylguanidine. J Med Chem. 1967; 10:833–840. [PubMed: 6057834]
5. Wieland DM, Brown LE, Tobes MC, Rogers WL, Marsh DD, Mangner TJ, Swanson DP, Beierwaltes WH. Imaging the primate adrenal medulla with [123I] and [131I] meta-iodobenzylguanidine: concise communication. J Nucl Med. 1981; 22:358–364. [PubMed: 7205383]
6. Taggart D, Dubois S, Matthay KK. Radiolabeled metaiodobenzylguanidine for imaging and therapy of neuroblastoma. Q J Nucl Med Mol Imaging. 2008; 52:403–418. [PubMed: 19088694]
7. Taggart DR, Han MM, Quach A, et al. Comparison of iodine-123 metaiodobenzylguanidine (MIBG) scan and [18F]fluorodeoxyglucose positron emission tomography to evaluate response after iodine-131 MIBG therapy for relapsed neuroblastoma. J Clin Oncol. 2009; 27:5343–5349. [PubMed: 19805691]
8. Sharp SE, Shulkin BL, Gelfand MJ, Salisbury S, Furman WL. 123I-MIBG scintigraphy and 18F-FDG PET in neuroblastoma. J Nucl Med. 2009; 50:1237–1243. [PubMed: 19617326]
9. Treuner J, Feine U, Niethammer D, et al. Scintigraphic imaging of neuroblastoma with [131-I]iodobenzylguanidine. Lancet. 1984; 1:333–334. [PubMed: 6141395]
10. Matthay KK, Shulkin B, Ladenstein R, Michon J, Giammarile F, Lewington V, Pearson AD, Cohn SL. Criteria for evaluation of disease extent by (123)I-metaiodobenzylguanidine scans in neuroblastoma: a report for the International Neuroblastoma Risk Group (INRG) Task Force. British Journal of Cancer. 2010; 102:1319–1326. [PubMed: 20424613]
11. Matthay KK, Yanik G, Messina J, et al. Phase II study on the effect of disease sites, age, and prior therapy on response to iodine-131-metaiodobenzylguanidine therapy in refractory neuroblastoma. J Clin Oncol. 2007; 25:1054–1060. [PubMed: 17369569]
12. Matthay KK, Quach A, Huberty J, et al. Iodine-131--metaiodobenzylguanidine double infusion with autologous stem-cell rescue for neuroblastoma: a new approaches to neuroblastoma therapy phase I study. J Clin Oncol. 2009; 27:1020–1025. [PubMed: 19171714]
13. Matthay KK, Tan JC, Villablanca JG, et al. Phase I dose escalation of iodine-131-metaiodobenzylguanidine with myeloablative chemotherapy and autologous stem-cell transplantation in refractory neuroblastoma: a new approaches to Neuroblastoma Therapy Consortium Study. J Clin Oncol. 2006; 24:500–506. [PubMed: 16421427]

14. Gaze MN, Chang YC, Flux GD, Mairs RJ, Saran FH, Meller ST. Feasibility of dosimetry-based high-dose 131I-meta-iodobenzylguanidine with topotecan as a radiosensitizer in children with metastatic neuroblastoma. Cancer biotherapy & radiopharmaceuticals. 2005; 20:195–199. [PubMed: 15869455]
15. Carlin S, Mairs RJ, McCluskey AG, et al. Development of a real-time polymerase chain reaction assay for prediction of the uptake of meta-[(131)I]iodobenzylguanidine by neuroblastoma tumors. Clin Cancer Res. 2003; 9:3338–3344. [PubMed: 12960120]
16. More SS, Itsara M, Yang X, et al. Vorinostat increases expression of functional norepinephrine transporter in neuroblastoma in vitro and in vivo model systems. Clin Cancer Res. 2011; 17:2339–2349. [PubMed: 21421857]
17. McCluskey AG, Boyd M, Ross SC, Cosimo E, Clark AM, Angerson WJ, Gaze MN, Mairs RJ. [131I]meta-iodobenzylguanidine and topotecan combination treatment of tumors expressing the noradrenaline transporter. Clin Cancer Res. 2005; 11:7929–7937. [PubMed: 16278418]
18. Moroz MA, Serganova I, Zanzonico P, et al. Imaging hNET reporter gene expression with 124I-MIBG. J Nucl Med. 2007; 48:827–836. [PubMed: 17475971]
19. Autret D, Bitar A, Ferrer L, Lisbona A, Bardies M. Monte Carlo modeling of gamma cameras for I-131 imaging in targeted radiotherapy. Cancer Biother Radiopharm. 2005; 20:77–84. [PubMed: 15778585]
20. Matthay KK, Panina C, Huberty J, et al. Correlation of tumor and whole-body dosimetry with tumor response and toxicity in refractory neuroblastoma treated with (131)I-MIBG. J Nucl Med. 2001; 42:1713–1721. [PubMed: 11696644]
21. Buckley SE, Saran FH, Gaze MN, Chittenden S, Partridge M, Lancaster D, Pearson A, Flux GD. Dosimetry for fractionated (131)I-mIBG therapies in patients with primary resistant high-risk neuroblastoma: preliminary results. Cancer Biother Radiopharm. 2007; 22:105–112. [PubMed: 17627418]
22. Lee CL, Wahnishe H, Sayre GA, et al. Radiation dose estimation using preclinical imaging with 124I-metaiodobenzylguanidine (MIBG) PET. Med Phys. 2010; 37:4861–4867. [PubMed: 20964203]
23. Gregory RA, Hooker CA, Partridge M, Flux GD. Optimization and assessment of quantitative 124I imaging on a Philips Gemini dual GS PET/CT system. Eur J Nucl Med Mol Imaging. 2009; 36:1037–1048. [PubMed: 19288099]
24. Hunter DH, Zhu X. Polymer-supported radiopharmaceuticals: [131I]MIBG and [123I]MIBG. J Labelled Cpd Radiopharm. 1999; 42:653–661.
25. Thompson J, Zamboni WC, Cheshire PJ, Richmond L, Luo X, Houghton JA, Stewart CF, Houghton PJ. Efficacy of oral irinotecan against neuroblastoma xenografts. Anticancer Drugs. 1997; 8:313–322. [PubMed: 9180383]
26. Dickson PV, Hamner B, Ng CY, Hall MM, Zhou J, Hargrove PW, McCarville MB, Davidoff AM. In vivo bioluminescence imaging for early detection and monitoring of disease progression in a murine model of neuroblastoma. Journal of pediatric surgery. 2007; 42:1172–1179. [PubMed: 17618876]
27. Iavarone A, Lasorella A, Servidei T, Riccardi R, Troncone L, Mastrangelo R. Biology of metaiodobenzylguanidine interactions with human neuroblastoma cells. J Nucl Biol Med. 1991; 35:186–190. [PubMed: 1823815]
28. Yu, AR.; Kim, JS.; Kim, KM., et al. Optimal PET acquisition setting of 1-124 with Siemens Inveon PET: Comparative simulation study with F-1 8 and microPET R4; 2009 IEEE Nuclear Science Symposium Conference Record (NSS/MIC); 2009. p. 2666-2668.
29. Loening AM, Gambhir SS. AMIDE: a free software tool for multimodality medical image analysis. Mol Imaging. 2003; 2:131–137. [PubMed: 14649056]
30. Stabin MG, Sparks RB, Crowe E. OLINDA/EXM: the second-generation personal computer software for internal dose assessment in nuclear medicine. J Nucl Med. 2005; 46:1023–1027. [PubMed: 15937315]
31. Waxler SH, Enger M. Organ weights and obesity in mice. J Nutr. 1954; 54:209–214. [PubMed: 13212459]

32. Barrett JA, Joyal JL, Hillier SM, et al. Comparison of high-specific-activity ultratrace 123/131I-MIBG and carrier-added 123/131I-MIBG on efficacy, pharmacokinetics, and tissue distribution. Cancer biotherapy & radiopharmaceuticals. 2010; 25:299–308. [PubMed: 20578835]

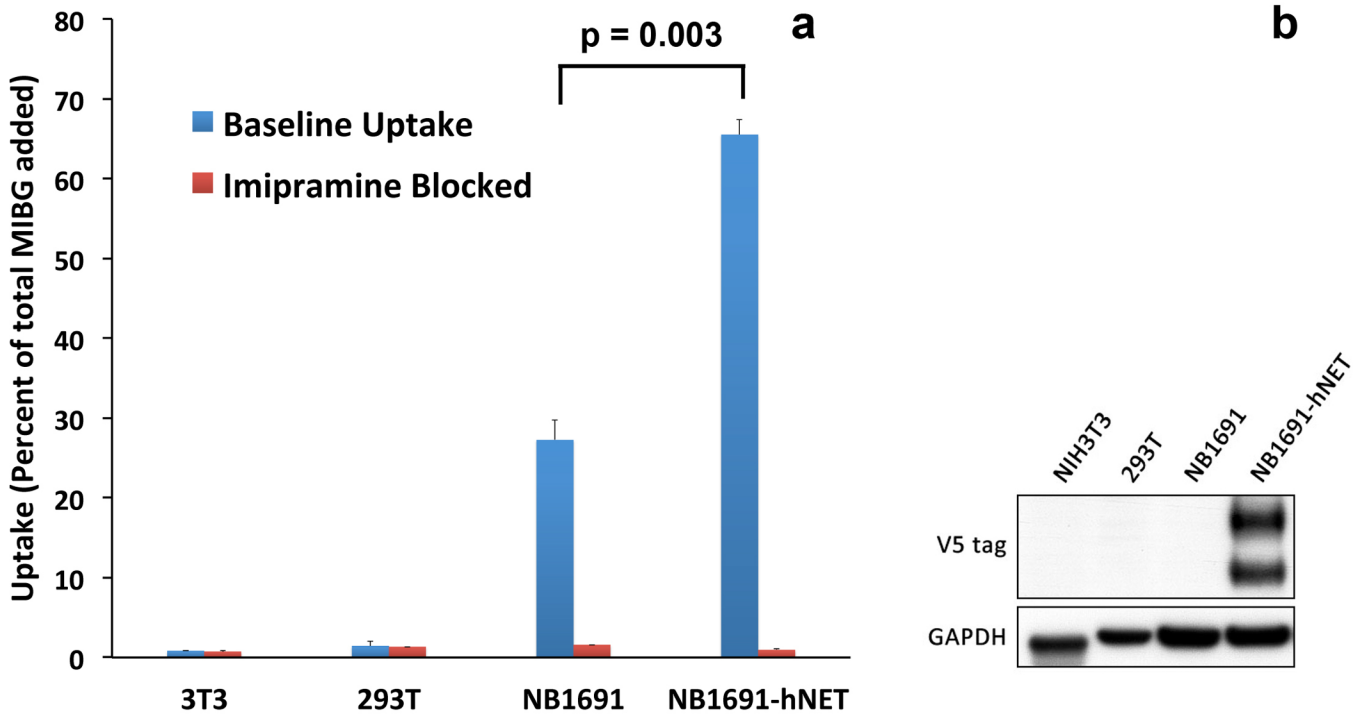

Fig. 1.

^{124}I-mIBG *in vitro* studies of cell association (binding or uptake) using unmodified NB1691, hNET-overexpressing NB1691 (NB1691-hNET), NIH 3T3, and HEK 293T cell lines as well as their corresponding cells blocked by imipramine, showing that ^{124}I-mIBG uptake is significantly higher in NB1691-hNET cells than in unmodified NB1691, NIH 3T3, and HEK 293T cells or in cells with blocked uptake. Western blot data (right) also show the enhanced hNET expression in the transduced NB1691 cells. The endogenous hNET is not evident in the western blot, which is only showing exogenously expressed, V5 tagged hNET. On the western blot data, amplification of glyceraldehyde 3-phosphate dehydrogenase (GAPDH) is used as a loading control and normalization.

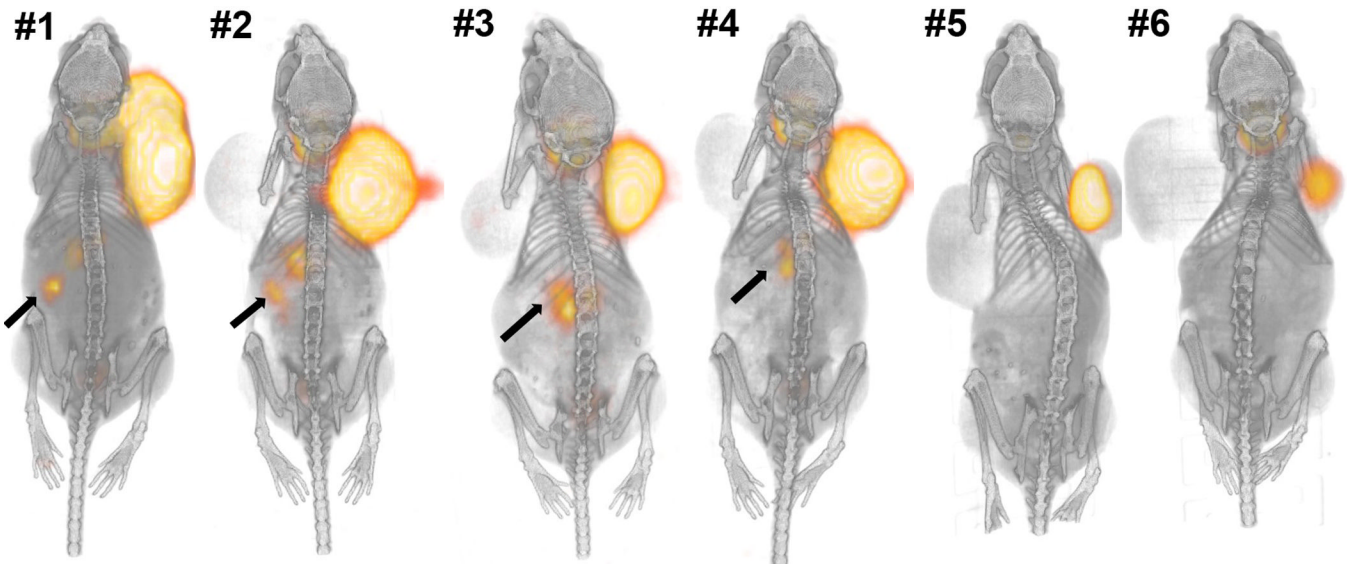

Fig. 2.

Six animals with subcutaneous (SubQ) NB1691 tumors on both shoulders presented as three-dimensional volume renderings of PET (orange color) overlaid on CT (gray-scale) images at 93–95 h after administration of ^{124}I-mIBG. The NB1691-hNET tumors (right shoulders) show significant uptake of mIBG, whereas unmodified NB1691 tumors (left shoulders) do not show any quantifiable ^{124}I-mIBG uptake. There is weak uptake (arrows) of ^{124}I-mIBG visualized in left kidneys of the first four animals (#1 – #4) where NB1691 cells were also injected. The first two (#1 and #2) were injected with hNET-overexpressing NB1691 cells, and the other two (#3 and #4) were injected with unmodified NB1691 cells.

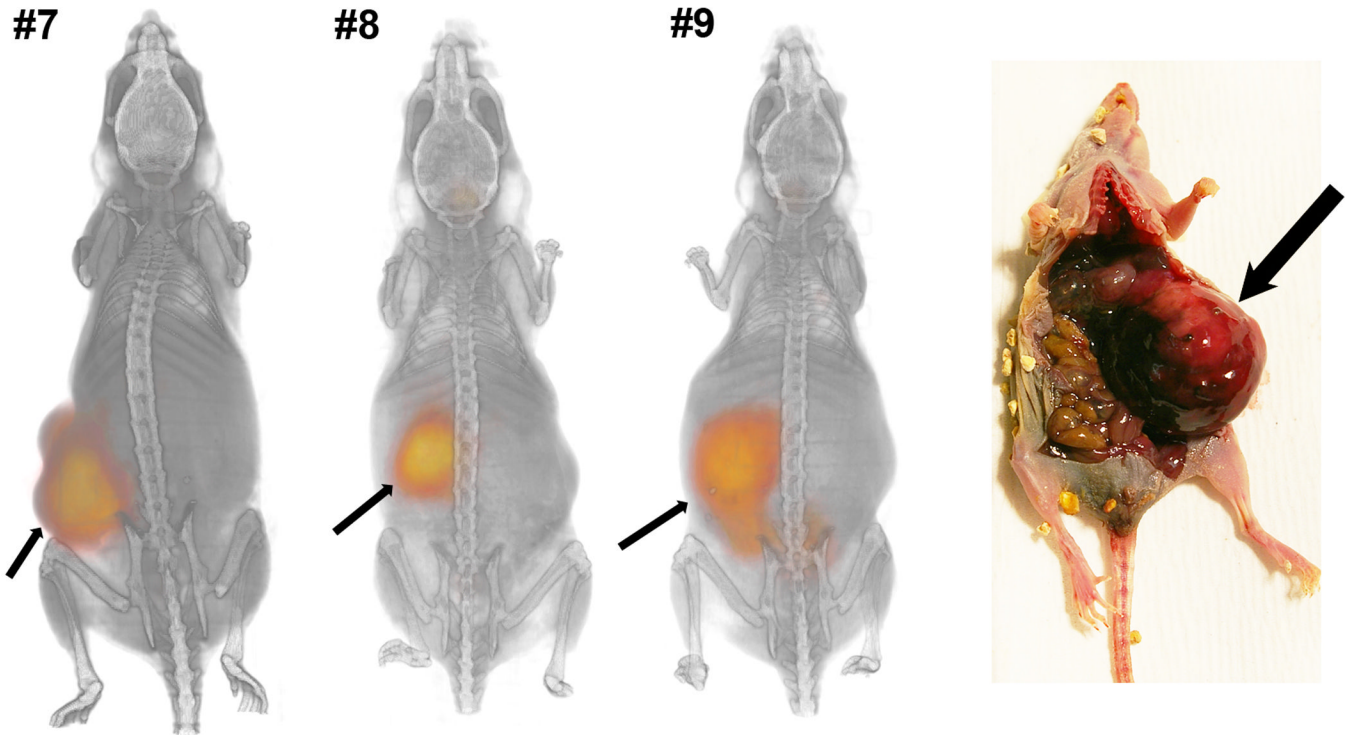

Fig. 3.

Three animals with hNET-transduced NB1691 tumors in the left renal capsules (RC) presented as three-dimensional volume renderings of PET (orange color) overlaid on CT (gray-scale) images at 93–95 h after administration of ^{124}I-mIBG. The hNET-overexpressing NB1691 tumors show significant uptake of mIBG. A photograph of tumors formed in the renal capsule and the corresponding tumor locations in PET/CT images (arrows) are shown in this animal model.

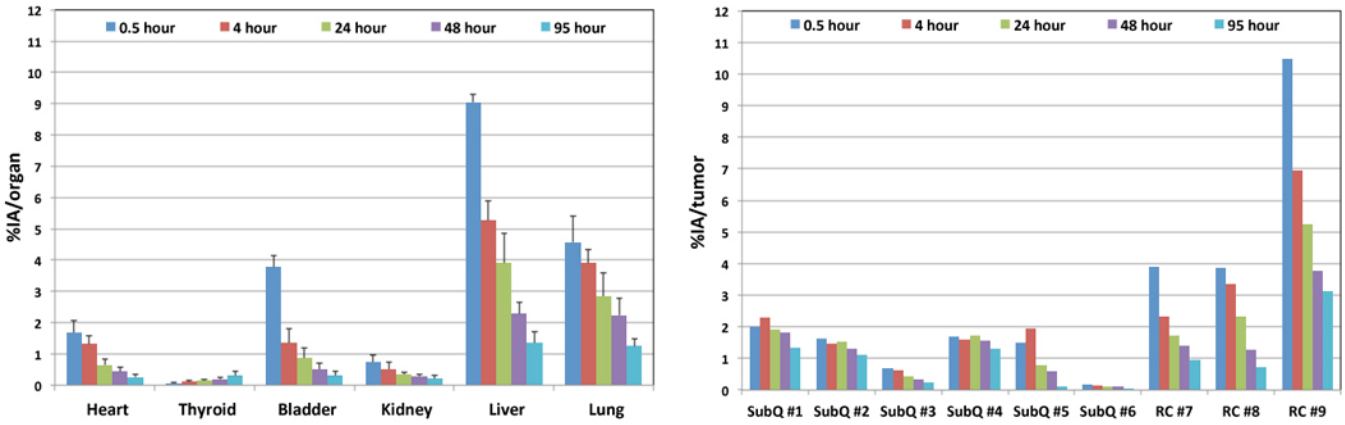

Fig. 4.

Biokinetic data of ^{124}I-mIBG uptake in heart, thyroid, bladder, kidney, liver, lung, and tumors (as shown in Figs. 2 and 3). Mean percent injected activity values and standard errors for the organs (%IA/organ) are shown as those extrapolated to the adult human-equivalent values. Percent injected activity values are shown for tumors (%IA/tumor) are shown without the extrapolation.

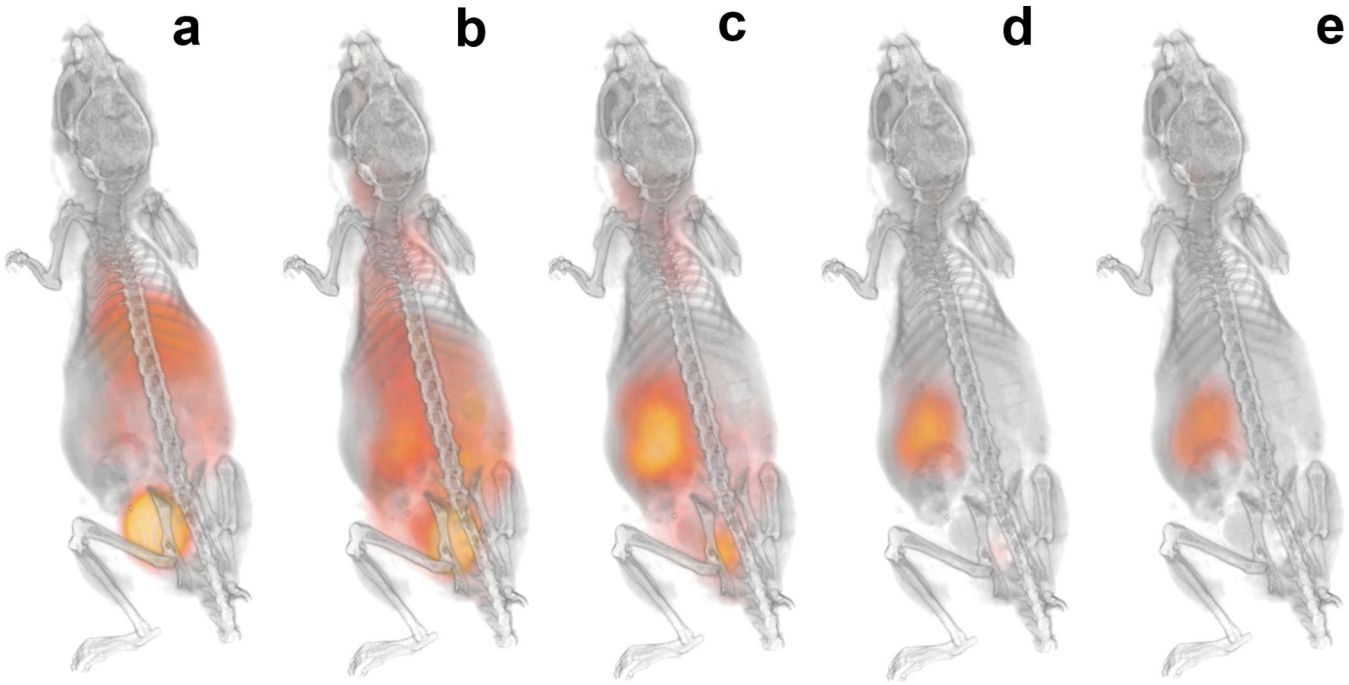

Fig. 5.

Representative PET/CT three-dimensional volume renderings at 0.5 (a), 4 (b), 24 (c), 48 (d), and 95 (e) hours after ^{124}I-mIBG administration. Temporal changes of mIBG uptake in whole-body are shown in the animal that has NB1691-hNET renal capsule tumor (#8 in Fig. 3).

Table 1

Normal organ dosimetry results and effective doses using ICRP 60 and ICRP 103 tissue weighting factors. The calculations show radiation doses extrapolated to those in adult human subjects using ^{124}I-mIBG data obtained from nine tumor-bearing mice.

Target organ	Subcutaneous (n=6)	Renal capsule (n=3)
	mSv/MBq	mSv/MBq
Adrenals	0.191±0.007	0.106±0.022
Brain	0.031±0.009	0.049±0.013
Breasts	0.052±0.006	0.065±0.017
Gallbladder Wall	0.105±0.008	0.120±0.026
LLI Wall	0.050±0.015	0.072±0.016
Small Intestine	0.053±0.012	0.076±0.018
Stomach Wall	0.059±0.009	0.079±0.020
ULI Wall	0.056±0.011	0.079±0.019
Heart Wall	0.355±0.069	0.301±0.080
Kidneys	0.238±0.075	0.228±0.061
Liver	0.348±0.145	0.318±0.059
Lungs	0.406±0.120	0.350±0.082
Muscle	0.049±0.009	0.066±0.016
Ovaries	0.053±0.015	0.075±0.017
Pancreas	0.082±0.008	0.100±0.023
Red Marrow	0.050±0.008	0.066±0.016
Osteogenic Cells	0.059±0.013	0.088±0.023
Skin	0.033±0.007	0.048±0.012
Spleen	0.058±0.008	0.078±0.018
Testes	0.038±0.012	0.057±0.013
Thymus	0.068±0.008	0.083±0.021
Thyroid	4.748±0.509	2.623±1.174
Urinary Bladder Wall	0.415±0.165	0.298±0.071
Uterus	0.068±0.020	0.084±0.014
Total body	0.065±0.008	0.083±0.015
Effective dose (ICRP 60)	0.351±0.027	0.238±0.061
Effective dose (ICRP 103)	0.332±0.024	0.240±0.055

Values are expressed as mean ± standard error of the mean.

Table 2

Tumor dosimetry results for the nine tumors with significant ^{124}I-mIBG uptake shown in Fig. 2 (SubQ #1-#6) and Fig. 3 (RC #7-#9). Tumor mass, ^{131}I-mIBG radiation dose estimate, and the amount of ^{131}I-mIBG to deliver therapeutic 20 Gy radiation to the tumor are listed.

Tumors (g)	^{131}I-mIBG dose (mGy/MBq)	^{131}I-mIBG (MBq) to deliver 20 Gy	^{131}I-mIBG (mCi) to deliver 20 Gy
SubQ #1 (0.755)	2.782×10^{2}	71.9	1.94
SubQ #2 (0.872)	1.811×10^{2}	110	2.97
SubQ #3 (0.226)	1.860×10^{2}	108	2.92
SubQ #4 (0.846)	2.300×10^{2}	87.0	2.35
SubQ #5 (0.193)	2.755×10^{2}	72.6	1.96
SubQ #6 (0.08)	9.714×10^{1}	206	5.57
RC #7 (0.687)	2.186×10^{2}	91.5	2.47
RC #8 (0.453)	3.790×10^{2}	52.8	1.43
RC #9 (1.844)	2.588×10^{2}	77.3	2.09